Contents lists available at ScienceDirect

Process Safety and Environmental Protection

journal homepage: www.elsevier.com/locate/psep

Deflagration of premixed methane–air in a large scale detonation tube

Mohammed J. Ajrash, Jafar Zanganeh, Behdad Moghtaderi*

The Frontier Energy Technologies Centre, Chemical Engineering, School of Engineering, Faculty of Engineering & Built Environment, University of Newcastle, Callaghan, NSW 2308, Australia

ARTICLE INFO

Article history:
Received 12 October 2016
Received in revised form 12 March 2017
Accepted 29 March 2017
Available online 8 April 2017

Keywords:
Methane deflagration
Detonation tube
Flame velocity
Dynamic pressure
Pressure wave
Flame intensity
Damage level

ABSTRACT

Methane explosion hazards in pipes are of pivotal concern in chemical plants. Accurate knowledge of flame deflagration and its behaviours are required to reduce the consequences of accidental fires and explosions. Considering a lack of experimental work exists in large scale methane-air deflagration systems, a detonation tube (30 m long) was facilitated at the University of Newcastle to cover the knowledge gap in terms of boosting flame deflagration of low methane concentrations and also examining flame deflagration characteristics with different reactive lengths (3, 6, 12 and 25 m). The feature of injecting methane at varied reactive sections (RS) was achieved using a balloon isolation system, a 50 mJ chemical ignitor used to ignite the initial explosion section. The results revealed that stagnation pressure gradually increased, from 2.03 bar to 3.77 bar then 4.57 bar, with increasing RS length from 3 m to 6 m then 12 m, respectively. There was no significant influence of 1.25% or 2.5% methane concentrations on dynamic or stagnation pressures, however, they extended the travelling flame distance by about 3 m for RS lengths of 12 m and 25 m. At 9.5% methane concentration and for a RS of 12 m a state of fast deflagration was observed, associated with 5 bar pressure rise. The pressure wave up to 6.5 m was only a few milliseconds (about 15 ms) ahead of the flame for almost the full methane concentration range, however, after this point the gap between the pressure wave and the flame significantly varied in accordance to the methane concentration, where the data analysis at 15 m indicated that for 9% methane concentration the flame was only 21 ms behind the pressure wave, and for 5% and 15% methane concentration the flame was behind the pressure wave in the range of 55–93 ms. Due to the limited length of the DT compared with the large volume of methane injected, there was no significant influence on the flame deflagration properties when extending the RS length from 12 m to 25 m, as the mixture initially located after 12 m pushed out through the open end.

1. Introduction

A pivotal concern of process industry safety is the prevention of potenial explosions. Understanding the criteria of the fire and explosion events and their consequences, however, is contributing to increasingly sophisticated design safety for the process industries (Eckhoff, 2013). As mining, oil and gas industry plants are typically congested, accidental fires and explosions are enhanced, causing massive loss of life and property. According to Khan and Abbasi (1999), there were about 2584 fatalities and 1800 injuries caused by chemical process accidents in the period between 1981 and 1997. Fugitive methane and natural gas (Oran et al., 2015) caused 279 fire accidents costing about $41 billion in property in the period between 1907 and 2007. As a part of these statistics, there were 2834, 3330 and 709 fatalities caused by coal mines, oil and gas industry fires and explosions, respectively (Sovacool, 2008). The majority of accidental fire and explosion events in coal mines

* *Corresponding author at*: C Block-NIER Building, University Drive, Callaghan, NSW 2308, Australia.
E-mail address: jafar.zanganeh@newcastle.edu.au (J. Zanganeh).
http://dx.doi.org/10.1016/j.psep.2017.03.035

are caused or enhanced by methane and natural gas, as reported by a number of researchers (Ajrash et al., 2016a; Akgun, 2015; Dhillon, 2010; Kundu et al., 2016; Lee, 2003; Lowesmith and Hankinson, 2013; Market et al., 2015; Tu, 2011; Wang et al., 2014). It is important to advise that 85%–99% of natural and fugitive gases consist of methane (Gamezo et al., 2012). An explosion is generally described as a sudden release of energy due to a chemical reaction with regard to the types of reactants (Ajrash et al., 2016b; Bai et al., 2011; Cashdollar et al., 2000; Eckhoff, 2013; Kundu et al., 2016; Sanchirico et al., 2011). In current research, the term explosion may refer to any combustion increase in the pressure of the system by 3% due to the fuel combustion, which may implicitly include both the deflagration and/or detonation (Ajrash et al., 2016c; Yuan et al., 2014).

1.1. *Methane air mixture explosions in cylindrical vessels*

Abel (1869) first discovered the pressure development of gases in tubes. However, Berthelot and Vieille (1881) were the first researchers who systematically measured the deflagration and detonation in tubes of hydrocarbon gases. Later, Mallard and Le Chatelier (1881) and Jouguet and Chapman (1913) theoretically and experimentally explained the phenomena of detonation in tubes. Mason and Wheeler (1920, 1917) are considered the earliest researchers to give attention to the characteristics of methane explosions in tubes. They observed that the flame velocity continually increased while traveling in the tube. The study was performed by using a laboratory scale setup with a tube of 50 mm diameter and 5 m long, closed at the ignition end, and open at the other end. In spite of using a relatively short tube and a small L/D ratio (3.65 m long and 0.305 m diameter), the phenomena of detonation was formed at stoichiometric methane air mixtures using a high energy explosive detonator, sodium chloride and ammonium nitrate (Payman et al., 1937). Kogarko (1958) also used higher energy explosive ignitors, a longer tube (11.2 m), and a similar diameter to the setup used by Payman et al. The most important conclusion was that the deflagration to detonation transition was observed in the range of 6.3%–13.5% of methane in air. In another study, the detonation present for methane concentration in the range of 8%–14.5% Wolanski et al. (1981).

Phylaktou et al. (1990) documented the flame speed and pressure rise rate for methane air mixture explosions in a vertical closed tube (1.64 m long, 21.6 L/D). Ignitors of 16 J were used and located at one end of the tube, with the pressure transducer mounted at the second end. To ensure a homogeneous mixture, an external circulation pump was used. Phylaktou et al. (1990) exhibited that at 10% methane, the pressure time history showed four phases. The first phase (short phase) represented the flame expanding from the ignitor. A rapid pressure elevation was noticed in the second phase, where the pressure increased from 1 to 3 bar in 30 ms. The third phase starts when the pressure rise and the flame speed are arrested and persist almost at constant values. The last stage was when the system suddenly cooled, and was associated with oscillations in the pressure readings. Finally, the pressure rise recoded was 6.9 bar when the equivalence ratio was equal to one (Phylaktou et al., 1990). Six one end open tubes with different diameters were used by Knystautas et al. (1982) to illustrate the influence of the tube diameter on the flame deflagration. The oxygen, nitrogen and fuel were introduced into the vacuum pressure system through a calibrated rotameter. The explosion was initiated through an exploding wire delivering 200–2500 J to the system.

The deflagration to detonation transition phenomena did not occur in all tubes at air stoichiometric conditions. Knystautas et al. extrapolated from β versus critical diameter that methane detonation may occur at the air stiochoimetric condition when the tube diameter is larger than 0.24 m. Kindracki et al. (2007) examined the effects of location of the initial ignition positions on the pressure rise of methane explosions in a horizontal tube 1.325 m long. Results were obtained for three concentrations, 7%, 9% and 12%. They also noticed that the position of the ignitor plays an important role on the flame speed and pressure profile, where the maximum pressure was recorded when the ignitors were in the middle of the tube. This was attributed to the fact that when the ignitor was at the end, a longer time is needed for the products to exchange the heat with the vessel walls.

The dynamic pressure of methane flame deflagration was highlighted by Wei et al., 2009. The experimental work was carried out on a 30 m long propagation tube with a 0.5 m diameter. Methane gas was used in the experiments, and each explosion was initiated by a 50 mJ chemical ignitor. The aim of the work was to address the static and dynamic pressure in a long propagation tube. Two approaches were used: firstly, the tube was fully open from one side; and secondly, the tube was closed by a structure. The two main outcomes could be summarized as follows: the maximum pressure of the experimental work was less than the theoretical estimations; and the measured values of the total pressure were very close to the theoretical values from the summation of the static and dynamic pressures. Additionally, there was no significant impact of the volume of the gases in the explosion on the static pressure when the tube was fully open.

In research work by Li et al. (2012), the interactions of methane flame velocity and the pressure wave were experimentally explored. The length of the tube was 12 m and the dimensions were 80 mm by 80 mm. A spark ignitor of 10 kJ was employed to ignite the methane air mixture. The results showed that the closed pipe had an obvious impact on the transition of the methane deflagration flame due to the pressure wave reflection. However, a number of researchers have studied the acceleration and the deflagration to detonation transition (Gamezo et al., 2012; Jiang et al., 2016; Kessler et al., 2010; Kuznetsov et al., 2002a, 2002b; Moen and Lee, 1982; Peraldi et al., 1988; Porowski and Teodorczyk, 2013; Salzano et al., 2002; Zipf et al., 2014). Other theoretical research has studied flame transport behaviour in vessels and tubes (Keshavarz and Oftadeh, 2002; Oran et al., 2011; Valiev et al., 2009; Wang et al., 2013; Zhang et al., 2011).

1.2. *Aim of the research*

The main aspect of this work is to cover the lack of experimental data on methane-air mixture deflagration in large-scale systems. The previous experimental work related to the topic could be criticized as follows; only few studies reported the methane flame deflagration in a large scale tube, most of them used a high energy ignition source that could overdrive the methane flame deflagration and give inaccurate results; And the values of dynamic and stagnation pressure were not reported in line with the flame deflagration properties. Finally, it has not been shown how low methane concentrations assist in accelerating flame deflagration of explosions in tubes. This case may be present in process and extractive industry (i.e. ventilation air methane), where the concentration of methane is typically less than 1.25%, but may rise up in abnormal conditions. The existing literature shows that there are only a few works previously highlighting the consequences and properties of methane-air mixture deflagration in a large-scale system. In 2015, a large-scale detonation tube system was built at the University of Newcastle (UoN) to cover the existing knowledge gaps needed to design a sophisticated capture duct able to trap and mitigate explosions and their consequences. The first aim of this work was to deliver valid data for the design of suitable mitigation and alarm systems. The second aim was to examine the propagation and deflagration of flames at low concentrations (below lean limit). Additionally, the study examines the front flame and pressure wave velocity results for variable tube explosion volumes. Finally, the static and dynamic pressures will be discussed for all of the above scenarios and expectations for the maximum destructive forces of varied methane concentrations under variable tube methane explosion volumes are given.

2. Experimental setup and methodology

2.1. *Detonation tube and diagnostics*

The detonation tube used in this study consisted of eleven sections with a diameter of 0.5 m, a total length of 30 m, and a 6 m silencer attached at the end of the tube to reduce the noise of the explosions (see Fig. 1).

Fig. 1 – Experimental setup at UoN.

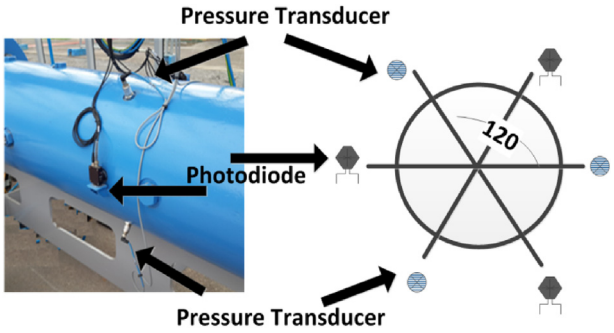

Fig. 2 – Pressure transducer and photodiode locations.

There were 33 pressure transducers and 33 photodiodes located along the length of the tube with three pressure transducers and three photodiodes located at the middle of each section. Each pressure transducer was located 120° out of phase from the nearest pressure transducer and each photodiode was located at 120° out of phase from the nearest photodiode. Each pressure transducer was offset 60° out of phase from the nearest photodiode but located in the same cross section plane as shown in Fig. 2. The pressure transducers pressure measurement range was 0–60 bar. The error reading was less than 0.25%, and the response time was <0.1 ms. The photodiodes had the following specifications: a reactive area of 13 mm^2, a wavelength range of 350–1100 nm, a rise time of 1 ns and a bias voltage of 10.6 V. The sampling frequency was set to 100 kHz (1 sample each 10 μs).

The DT sections generally divided to three types, initial ignition (explosion) chamber with chemical ignitor (Section 1), Reactive Section RS: Section in which different methane concentrations were present; The RS length was adjusted according to the case scenarios, and Non-Reactive Section NRS: Section filled only with air; The NRS length was adjusted according to the case scenarios, see Figs. 3 and 4. Balloon isolation systems were used to separate the RS from the NRS of the DT. A blowing system was used to purge the air inside the DT. The temperature of the reactive system was recorded by a pyrometer at a frequency of 100 kHz through a sapphire window. A high speed colour camera (type Phantom 4) was set at 2000 fps and a video camera was mounted at the initial RS (type Bazlar, set at 255 fps).

2.2. *Gas mixture*

The homogeneity of the methane-air mixture was achieved by two circulation systems along the tube. Each circulation system consisted of a blower (the volumetric flow rates for the first and second circulation blowers were 720 l/min and 1900 l/min, respectively). There were four pneumatic valves, two methane monitors, a flame arrestor and a rotameter in each system. For each system there was a methane line connected to a methane cylinder via two pneumatic valves and a mass control flowmeter (see Fig. 3).

Table 1 – Balloon sealing system locations.

	First sealing system	Second sealing system	RS length (m)
Case 1	Sect. 2	Sect. 3	3
Case 2	Sect. 2	Sect. 4	6
Case 3	Sect. 2	Sect. 6	12
Case 4	Sect. 2	Sect. 11	25

The methane–air mixture in the detonation tube was ignited in four cases (see Fig. 4). In all cases, the ignition chamber was fuelled with a stoichiometric methane-air mixture. The explosion characteristics, pressure wave and flame velocities were investigated for a wide range of methane-air mixtures (1.25%, 2.5%, 5%, 7.5%, 10% and 15%). The four configurations are shown in Fig. 4.

2.3. *Procedure*

The system was designed to be operated from a control room located about 30 m away from the explosion chamber. To conduct the test, firstly, the system was purged with fresh air by activating the purging system (an air blower and two pneumatic valves). Then, the ignitor was loaded at the beginning of the first section. The sealing step was varied depending on the scenario and case number. There were two balloon sealing systems, the first one was permanently located at the beginning of Section 2 and the second sealing system was adjustable depending on the case number; For instance Fig. 4, the sealing system was relocated from the beginning of Section 4 to the beginning of Section 6 (for more information please see Table 1).

The balloon sealing system consisted of a pneumatic valve, a manual valve, a portable pump and a balloon that was replaced after each test. The concept of sealing is to inflate a balloon inside the tube to isolate the upstream from the downstream of the balloon sealing system. The next step after sealing the sections was to evacuate the site. The system was remotely controlled from the control room outside the DT area. All of the sensors were activated at the time of ignition for the measurement of the pressure, temperature and the

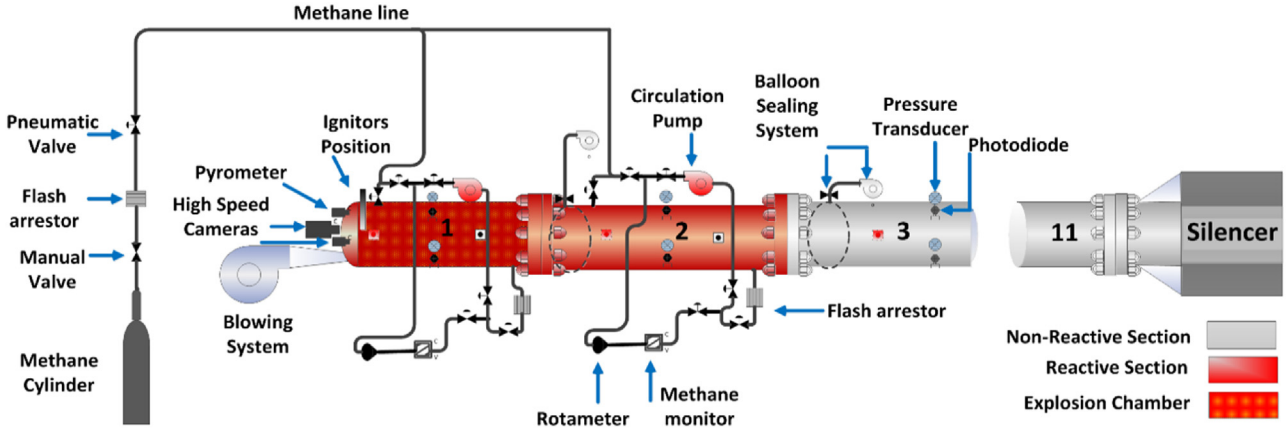

Fig. 3 – Components of detonation tube at UoN.

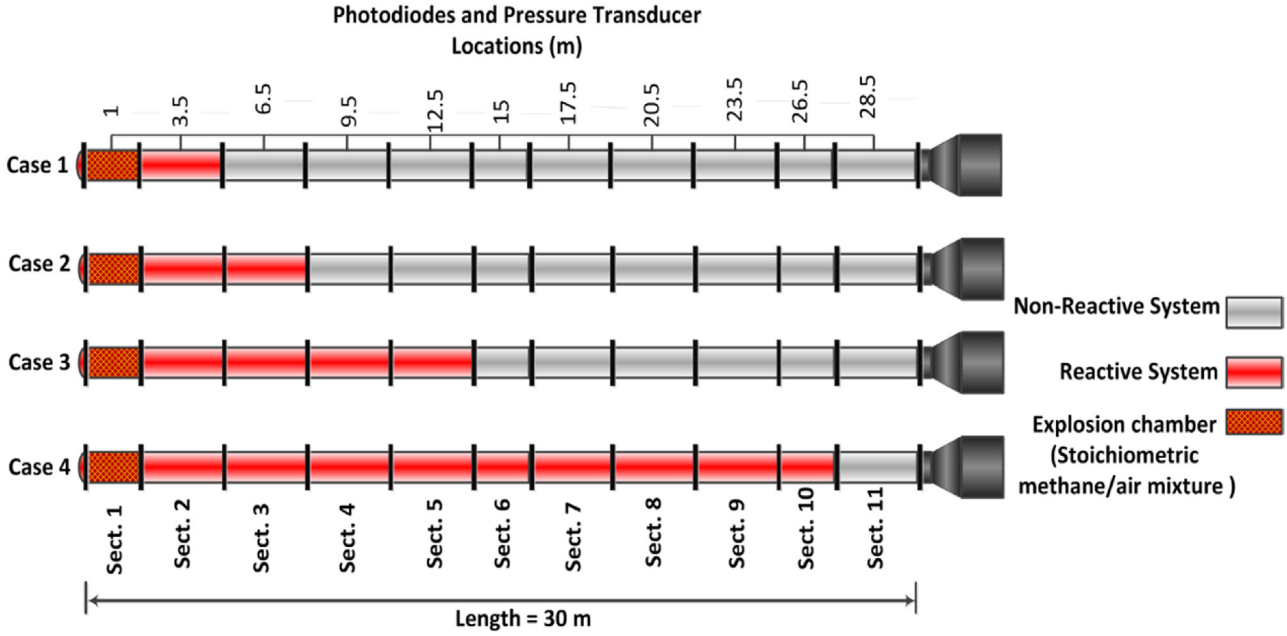

Fig. 4 – Demonstration of four case scenarios.

detection of flame. The data was automatically saved on the logging and control computer. Finally, the system was purged with air after the test was completed.

3. Results and discussion

3.1. *Initial explosion*

As discussed in Section 2.3, the initial explosion was initiated by an explosion of 9.5% methane at the first spool. The explosive mixture was ignited by a 50 mJ chemical ignitor. The static pressure, flame and temperature of the initial explosion are shown in Fig. 5.

The pyrometer was adjusted to measure the temperature at the end of the initial explosion section (Section 1). The aim of the pyrometer calibration was to record the actual temperature the flame reached in the active section. Fig. 5 shows the combustion of methane at about 25 ms, where it was clearly detected by both the temperature profile and flame intensity. The maximum pressure rise recorded was 0.6 bar, and the maximum flame intensity signal recorded was 1.7 V at about 75 ms, the flame intensity is represents the direct reading of the photodiode signal. The maximum temperature recorded was about 900 °C. The pressure wave velocity and the flame velocity values were 35 m s^{-1} and 29 m s^{-1}, respectively. These values were calculated according to the distance from the location of the ignitors to the first set of pressure transducers and photodiodes. Finally, the pressure rise was present along the DT. However, the flame tracking showed the flame diminished and disappeared at 9.5 m.

3.2. *Maximum pressure rise*

Addressing pressure rise is an important parameter in characterising explosion hazards. The maximum pressure rise in pipes relies on the distance from the ignition source, the initial conditions, ignition source energy and location, L/D ratio, the flammable gas concentration and the distance the flame travels. When an ignition source ignites a gas, the pressure from the explosion is a measure of the exertion of stress in all directions surrounding the ignition source. The propagation of explosions is measured by three types of pressure, static, dynamic and stagnation pressure. The static pressure is imposed on the side of the tube in a perpendicular direction from the flame propagation direction. The static pressure may be referred to as side on pressure. The dynamic pressure

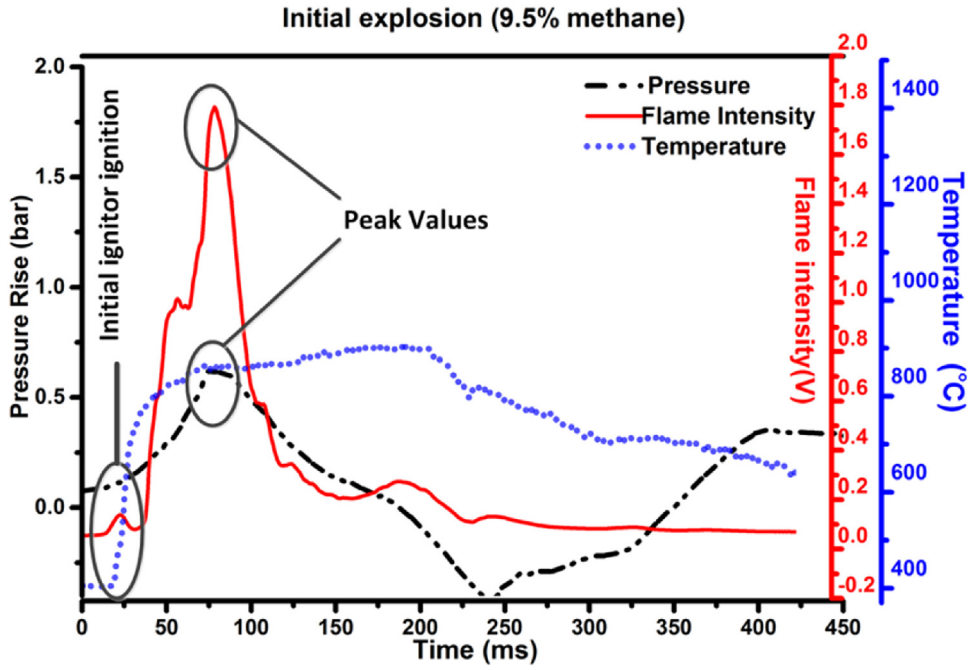

Fig. 5 – Pressure, flame intensity signal and temperature of the initial explosion.

represents the pressure that the moving fluid would have in the head of propagation (Bjerketvedt et al., 1997). The dynamic pressure, P_{Dyn}, is expressed as the following:

$$P_{Dyn} = \frac{\rho u^2}{2} \quad (1)$$

where ρ is the fluid density and u represent the velocity.

The summation of both the static and dynamic pressures is called the stagnation pressure, which is mathematically expressed by the following equation:

$$P_{Stag} = P_{St} + P_{Dyn} \quad (2)$$

In this work, the dynamic pressure was detected via two Pitot tubes located at 28 m from the ignition source, and the stagnation pressure was calculated according to Eq. (2).

In this section the static, dynamic and stagnation pressures were addressed to illustrate the consequence of methane explosions in a chemical plant and coal mine For example, prediction of the damage to structures, prediction of the fluid velocity from the dynamic pressure and to consider the impact of the stagnation pressure when designing both a structure and a mitigation system. The static, dynamic and stagnation pressures are shown in Fig. 6.

The results showed that the dynamic pressure was higher than the static pressure in all cases and in all the methane concentrations of the experimental works (see Fig. 6). The maximum values of the static, dynamic and stagnation pressures were at 9.5% methane concentration. This adds to evidence that 9.5% represents the stoichiometric value of methane in air explosions (Ajrash et al., 2017; Amyotte et al., 1991; Bai et al., 2011; Cashdollar et al., 2000, 1992). The maximum value of the static pressure for the 3 m active section and the 6 m active section did not exceed 0.6 bar (see Fig. 6(a) and (b)). However, the static pressure reached to over 2 bar for the 12 m active section and the 25 m active section. This may be attributed to the fact that at the 3 m and 6 m RS lengths, the flame did not reach the end of the tube. However, as the length of methane injection increased to 12 m and 25 m, the flame reached to the last section of the DT (30 m) and significantly increased the static pressure. The dynamic pressures for all four cases at low methane concentrations (1.25%, 2.5% and 5%) were about 0.5 bar. In the case of low methane concentration (i.e. 1.25% and 2.5%), the reading of dynamic pressures were over driven by the initial explosion in the first section. In other words, the low methane concentration did not have a pronounced influence on the pressure values, and the pressure values were generated mainly from the initial explosion chamber. At 7.5% methane, the dynamic pressure proportionally increased in accordance with the length of RS, where the dynamic pressure increased from about 0.95 bar to 1.5 bar for the 3 m and 6 m RS, respectively. The dynamic pressure continually increased until reaching a maximum value (2 bar) at the 25 m RS. At the stoichiometric methane concentration (9.5%), the dynamic pressure significantly increased, from 1.4 bar to 2.2 bar, then to 2.56 bar, when increasing the RS from 3 m to 6 m, then to 12 m, respectively. However, the value of dynamic pressure was fixed at about 2.55 bar, even when increasing the RS length to 25 m (see Fig. 6).

The static and dynamic pressure at low methane concentrations were over driven by the initial explosion and almost constant dynamic and static pressures were recorded. Therefore, the stagnation pressure did not show any significant change at low methane concentrations, where the stagnation pressure values varied around 1 bar for all cases at low methane concentrations (see Fig. 6). At 9.5% methane concentration, the stagnation pressure dramatically increased from 2 bar to 4.5 bar when increasing the RS length from 3 m to 12 m, respectively. In a similar behaviour to the static and dynamic pressures, increasing the length of the RS, from 12 m to 25 m, did not show a significant impact on the stagnation pressures.

3.3. *Flame and pressure wave characteristics*

The explosion energy appears in a number of forms. The major energy of an explosion appears in a pressure wave form (Frank, 2012). The remaining energies appear in both potential and

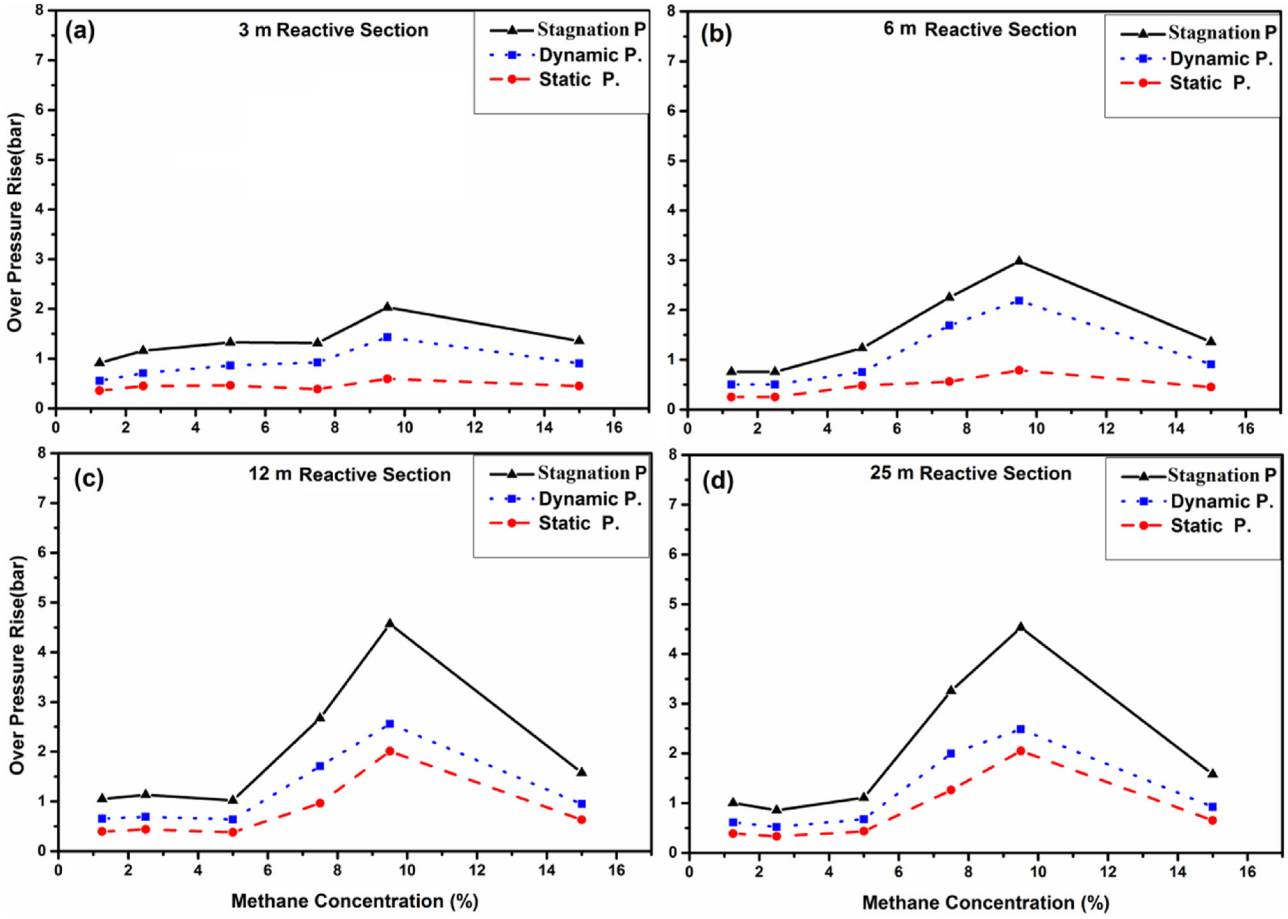

Fig. 6 – Static, dynamic and stagnation pressures for (a) Case 1, (b) Case 2, (c) Case 3 and (d) Case 4.

kinetic forms. The destruction from an explosion propagating in pipes depends on the pressure rise and the impulse generated from the flame deflagration (Otsuka et al., 2007). A detailed record of methane flame deflagration velocity is not only required to determine the pressure impulse and explosion development, but also to design an effective flame mitigation system. The flame velocity helps to estimate the distance and time required between the flame detectors and the location where the flame mitigation acts. The terminology of "flame velocity" is conventionally defined as the velocity of the flame relative to a stationary point. The scholars assumed that the boundary condition of a gas's velocity ahead of the flame is identical to the first indication of a flame reaching a photodiode. Another group of scholars measured the flame velocity relative to a stationary point. the velocity was calculated as the time and length from ignition point to the first increased point of temperature, where the assumption was the first increased point of the temperature is asymptotic to the point of the gases ahead of the flame (Frank, 2012; Gunther and Janisch, 1972; Tien and Matalon, 1991). The flame velocity is mathematically descried as:

$$S = U + u_g$$

where S ($m\,s^{-1}$) is the flame velocity, U ($m\,s^{-1}$) is defined as the burning velocity, the velocity of the front flame relative to unburnt gas, and u_g ($m\,s^{-1}$) is the velocity of the unburnt gas (see Fig. 7).

The pressures in detonation phenomena may increase by up to ten times that of the initial explosion. In the next section, the pressure wave profiles, pressure wave velocities and

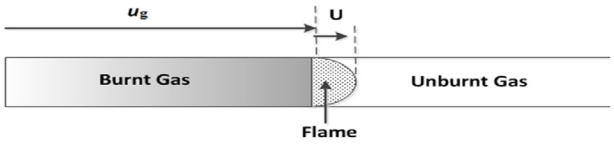

Fig. 7 – Illustration of the flame velocity in a tube (Bjerketvedt et al., 1997).

destruction levels are discussed according to the RS length (see Table 1).

3.3.1. *Pressure wave profiles*

The pressure wave profiles showed similar behaviours for concentrations below the lower flammability limits (1.25%, 2.5% and 5%) and at the rich limit (15%). For the 3 m RS, the pressure wave travelled at about 0.8 bar pressure until 15 m from the ignition source. Then the pressure wave gradually declined to about 0.4 bar at about 28.5 m from the ignition source. However, the pressure wave for 5% and 15% at the 25 m RS travelled for about 23.5 m at the same energy (1 bar) before declining. Fig. 8 shows clearly that for both scenarios (the 3 m and 25 m RS) the pressure wave of 9.5% is much higher than for 5% and 15% methane concentrations. It is clearly explicit that the initial explosion has a major impact on the travelling pressure wave, and is in agreement with (Blanchard et al., 2011; Frank, 2012; Moen and Lee, 1982; Rasbash and Rogowski, 1960).

For 9.5% methane concentration and the case of a 3 m RS, the pressure wave also started to diminish at a distance of 23.5 m (similar to 5% and 15% methane concentrations at the 3 m RS). In contrast, the pressure wave for a 9.5% methane concentration at the 25 m RS showed a distinct behaviour,

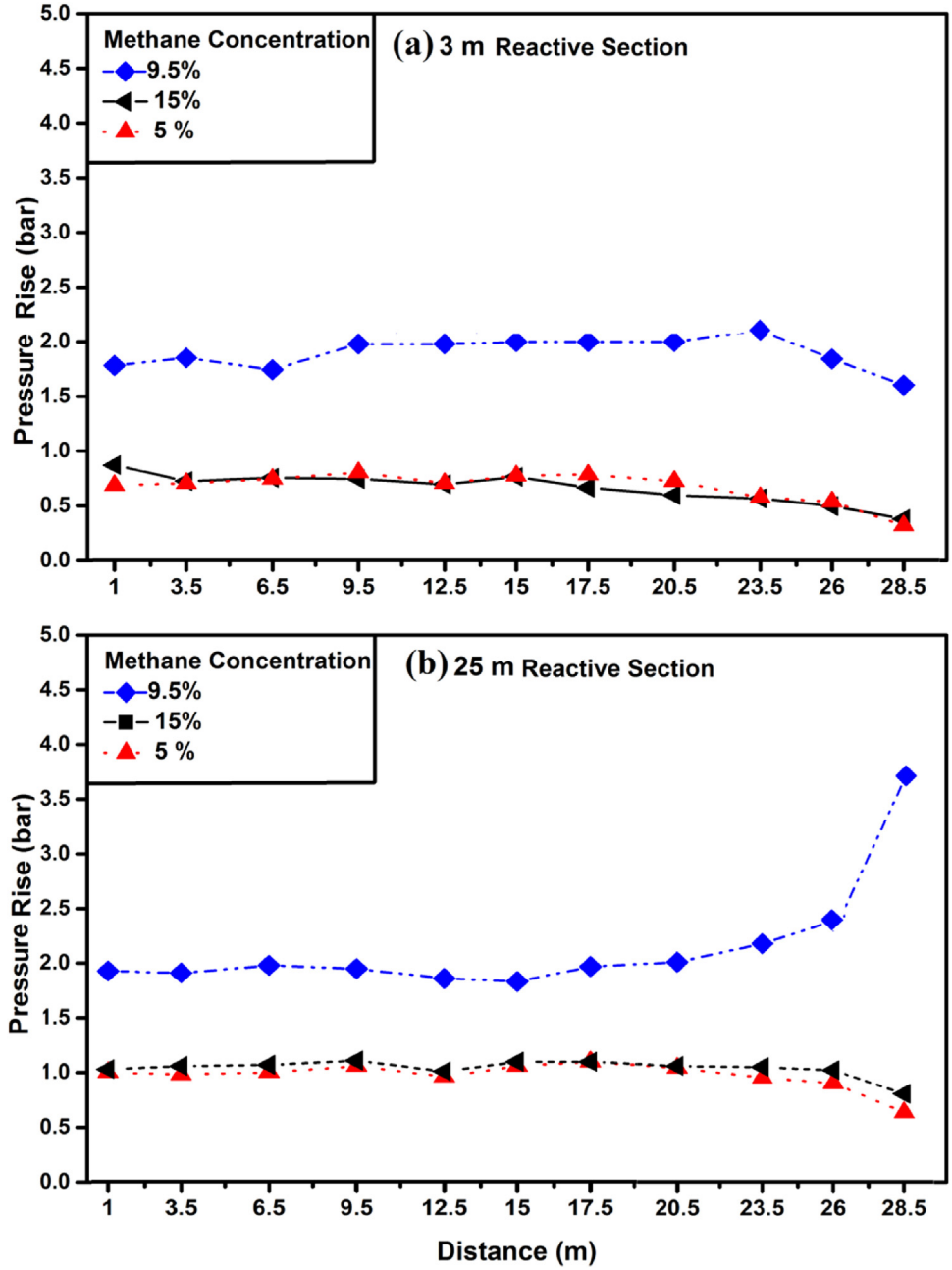

Fig. 8 – Pressure wave profiles for 5%, 9.5% and 15% methane concentrations for (a) 3 m RS and (b) 25 m RS.

where the pressure profile continually increased from 20.5 m until the end of the tube (from 2.05 bar at 20.5 m to 3.8 bar at 28.5 m). The pressure developed and the shape of the pressure profile appeared only for 9.5% methane concentration. The development of pressure at 9.5% methane concentration is attributed to the accelerating flame; as a result, the value of pressure will increase as the volume of the product gases increase. The flame interaction with the pressure wave of 9.5% methane concentration is clarified in Section 3.3.4.

Another influence of the RS length on the pressure wave profile appears for 7.5% methane concentration (see Fig. 9). The analysed data showed that for the 3 m RS, the explosion initiated a 1.4 bar pressure wave which travelled for about 20 m. Then, the pressure wave declined gradually to 0.4 bar, where the pressure wave profile behaved in a typical way to the observed methane explosion at the 3 m RS length (see Fig. 9). The pressure wave profiles of 7.5% methane concentration at the 6 m and 12 m RS showed a slight development in the pressure wave. This behaviour does not appear for the explosion of methane at the lower flammability concentration limit, or below, for all four RS lengths. The peak of the developed pressure wave was stronger for the 25 m RS. However, all the pressure developed then declined after 23.5 m, and did not develop to detonation. The first symptoms of pressure developing occurred between 9.5 m and 12.5 m from the ignition source for the of RS lengths of 6 m, 12 m and 25 m.

The rapid increase in the pressure of the pressure wave is attributed to the increased burning rate. Nonetheless, the value of the developed pressure is directly proportional to the RS length, where the pressure wave mainly depends on the amount of product gases and, eventually, the burning rate.

To sum up, three patterns of pressure waves were observed in the current experimental work. The first pattern was a distinct behaviour for the 3 m RS for all methane concentrations. The pressure wave travelled at a pressure close to the initial pressure rise for a specific distance, then gradually dimin-

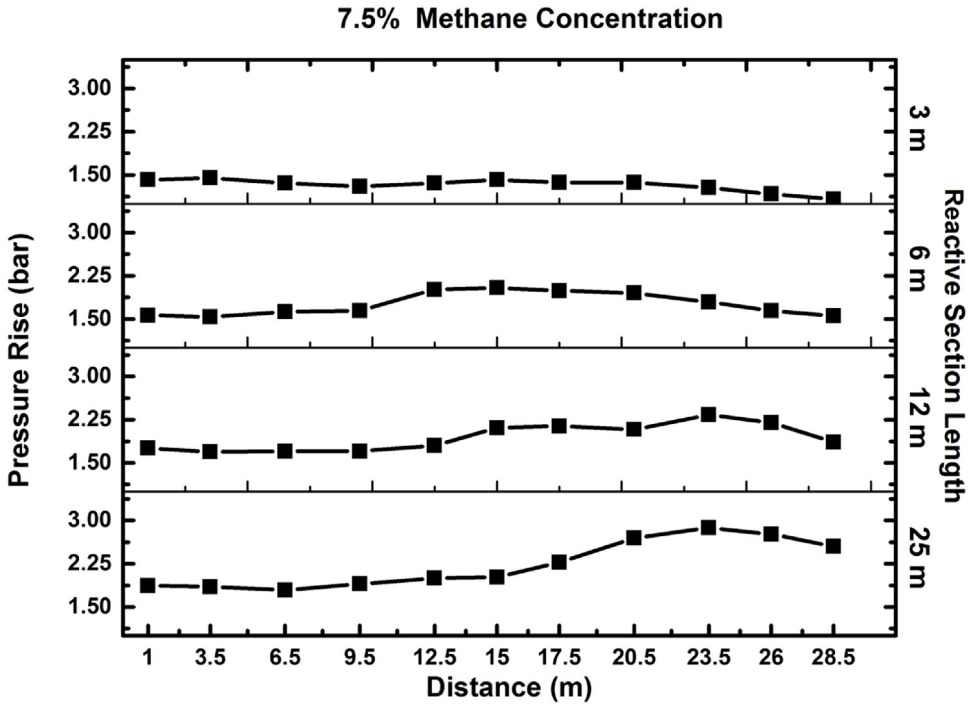

Fig. 9 – Pressure wave profiles for 7.5% methane concentration.

ished. The second pressure wave pattern showed the pressure developing after a specific distance. The peak value of the pressure wave was strongly dependant on the run up distance. The previous pattern was distinct for 7.5% methane concentration for the last three RS length cases (6 m, 12 m and 25 m), and the behaviour also appears at 9.5 m for the 6 m RS. The last pressure wave pattern showed a fast development at the end of the tube. This behaviour appeared at the methane stoichiometric concentration for the 25 m RS. The pressure wave patterns have good agreement with (Bjerketvedt et al., 1997).

3.3.2. *Pressure wave velocity*

Another factor which determines the pressure wave properties is the pressure wave velocity. The pressure wave velocities were calculated relative to the ignition point (stationary point). The data revealed that the pressure wave velocities for stoichiometric methane concentrations, and below, were affected by the pressure rise, and eventually by the burning rate. At a rich methane concentration (15%), nonetheless, the pressure wave velocity was relatively high, as compared to the pressure rise of a 9.5% methane concentration.

The pressure wave velocities for all four cases of RS lengths gradually increased until the last section of the DT. In a similar behaviour to the pressure rise profile, Fig. 10 shows the pressure wave velocities for the 3 m RS and the 25 m RS. It was found that when increasing the RS length, the velocity of the pressure wave increased, even at a distance of 1 m. For instance, for a 9.5% methane concentration and at a 3.5 m distance, the pressure wave velocity increased from 40 m s^{-1} to 145 m s^{-1} as the length of the RS was increased from 3 m to 25 m. The maximum pressure wave velocity was 310 m s^{-1} for methane stoichiometric concentration at 9.5 m, and the minimum pressure wave velocity was 25 m s^{-1} at 5% methane concentration for the 3 m RS (see Fig. 10).

3.3.3. *Flame profile*

Chemical energy is the form of the energy released from an explosion. In pipes, the combustion of the flammable gases (flame propagation) characterises the explosion propagation. The design of a mitigation system requires accurate data for the flame travel distances and the flame velocities in all possible scenarios. In this work, and in correspondence to the identified knowledge gaps, the experimental flame travel distances and flame speeds were measured for six methane concentrations under each of the four RS lengths.

Table 2 – Flame travel distances for the four RS length cases.

Methane concentrations	RS Length			
	3 m	6 m	12 m	25m
1.25%	9.5	9.5	12.5	23.5
2.5%	9.5	12.5	12.5	23.5
5%	12.5	15	15	23.5
7.5%	23.5	28.5	28.5	28.5
9.5%	23.5	28.5	28.5	28.5
15%	15	20.5	17.5	23.5

The flame travel distances for all RS length cases are shown in Table 2. As extrapolated before, the data for the 1.25% and 2.5% concentrations for the 3 m and 6 m RS was over driven by the initial explosion. For these concentrations, the flame travel distances were about 9.5 m from the ignition source. The flame travel distance for the 1.25% and 2.5% concentrations, nonetheless, travelled for 12.5 m and 23.5 m for the 12 m and 25 m RS lengths, respectively. The flame travel distance for 5% methane concentration was about 50% higher than for 2.5% methane concentration. Additionally, the flame travel distance of methane at its stoichiometric concentration was about threefold that of 2.5% methane concentration at the 3 m RS length. Finally, only the flame with 6 m RS length reached the last section of the DT for 7.5% and 9.5% methane concentrations. The most powerful detection approach to a fire in a chemical plant is through sensoring the light, temperature and pressure. Photodiodes are the primary detection system to activate the mitigation system and/or fire alarms. Gaining a good understanding of the flame intensities along

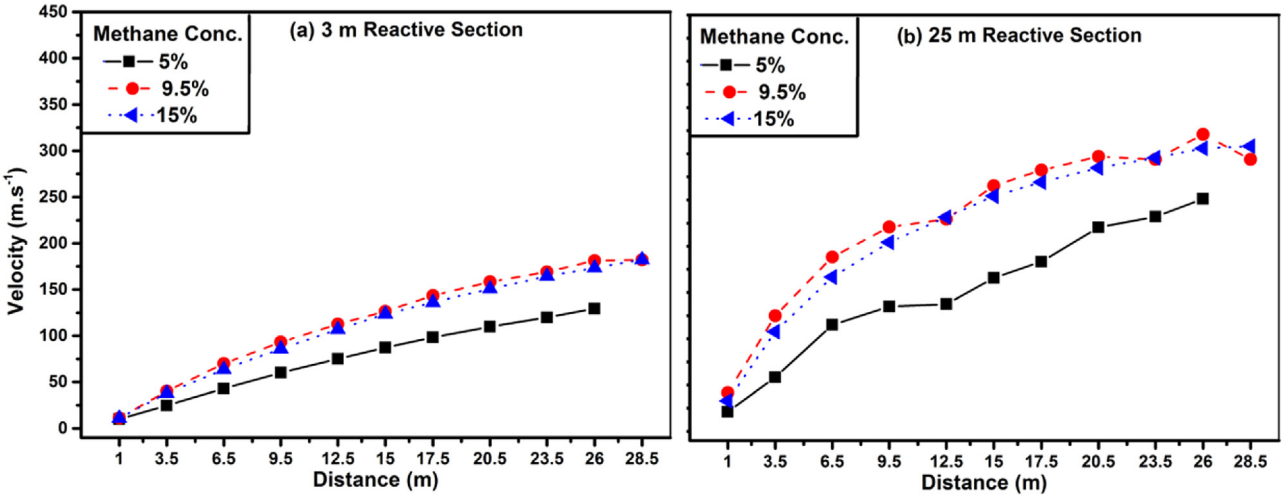

Fig. 10 – Pressure wave velocities for (a) 3 m RS and (b) 25 m RS.

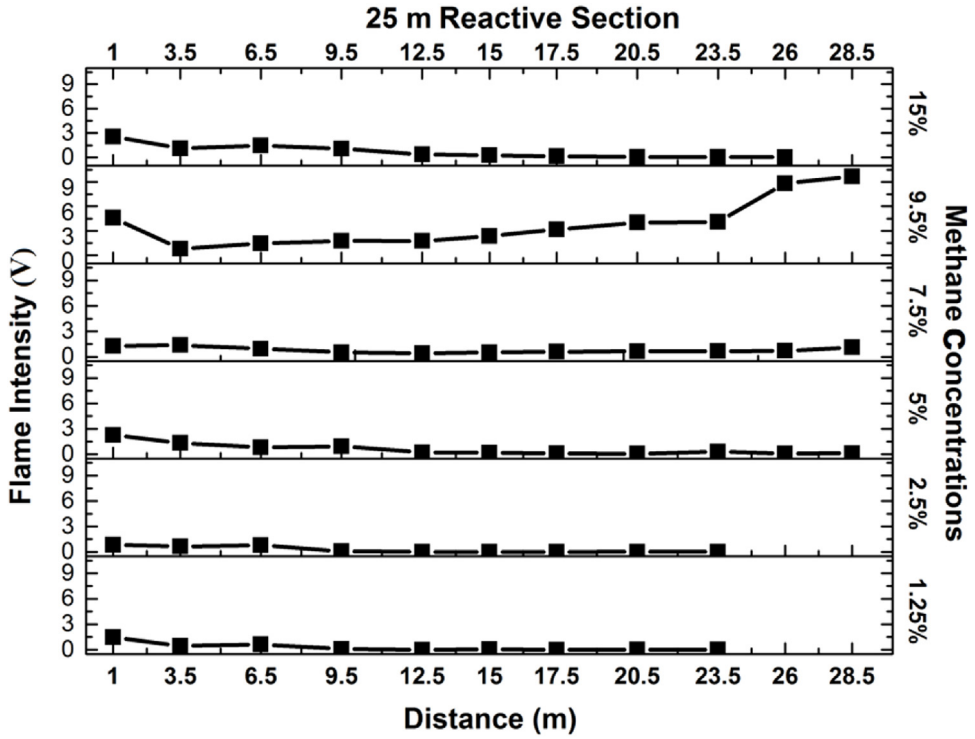

Fig. 11 – Flame intensity signals for 25 m RS length.

the detonation tube gives a clear indication of the minimum flame intensity signal that could be present during a flame proprogation.

The photodiodes gave a reading up to 10 V (see Section 2.1), and any reading below 0.03 V in this work was considered as noise due to a pressure rise or light reflection from the flame in the prior sections. Fig. 11 shows the flame intensity signals for the 25 m RS length at 1.25%, 2.5%, 5%, 7.5%, 9.5% and 15% methane concentrations.

The first photodiode data (at 1 m distance) represents the reading of the initial explosion chamber. The flame intensity signal of the first section ranged between 1.5 V to 3 V. Regardless, the methane concentration in the RS, exempting the 9.5% scenario, caused the flame intensity signal in the first section to reach about 4.5 V. The flame tracking of the 1.25% and 2.5% methane concentrations, notwithstanding, caused the flame to be detected at about 23.5 m, as compared to only 9.5 m when the RS was free of methane. The detected flame intensity signal of the 1.25% and 2.5% methane concentrations was 0.05 V. The flame travelled until the last section of the DT when 5%, 7.5% and 9.5% methane concentrations were used in the RS. The lowest flame intensity was detected for the 5% and 7.5% methane concentrations at about 0.09 V. The flame intensity signal of the stoichiometric concentration was much higher (0.9 V–9.6 V). The high flame intensity signals detected may be attributed to the turbulence of the flame at stoichiometric conditions. Finally, the flame travel distance at a rich methane concentration (15%) failed to reach the end of the tube at the last detector at 26 m (0.4 V).

3.3.4. *Flame velocity*

The flame velocity was calculated relative to the first sign of the flame light detection (0.05 V). Fig. 12 illustrates the methane flame velocities for three methane concentrations (5%, 9.5% and 15%). The outcomes indicated that the highest flame velocity for the 3 m RS length was about 120 m s^{-1}. At

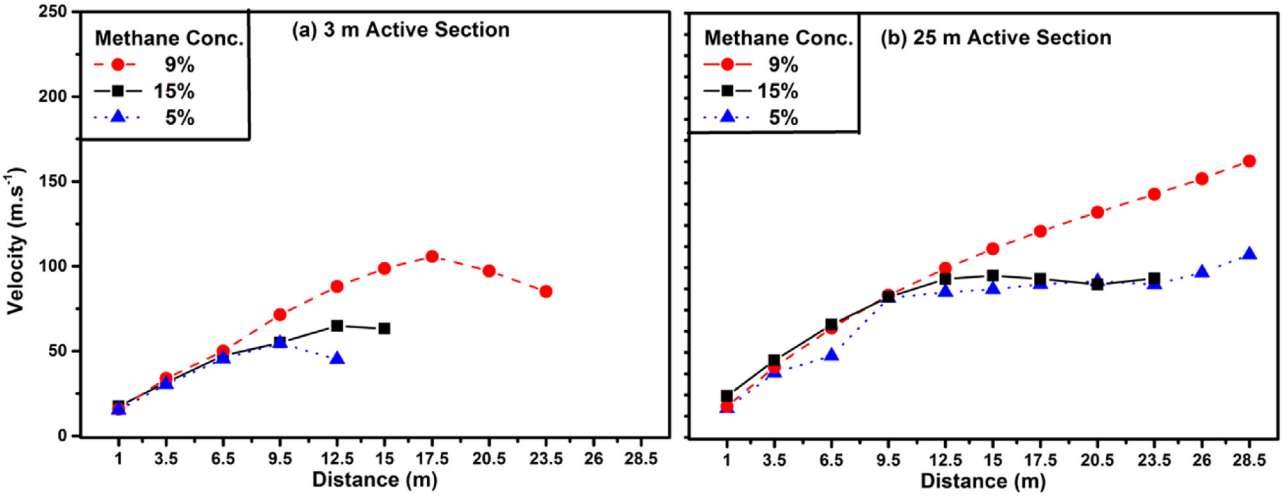

Fig. 12 – Flame velocities for 5%, 9.5% and 15% methane for (a) 3 m RS and (b) 25 m RS.

a stoichiometric methane concentration (see Fig. 12(a)), the peak velocity was achieved at 17.5 m before the flame velocity began to decline. For 15% methane concentration, the peak flame velocity (70 m s^{-1}) was achieved at a distance of 12 m. However, the lowest peak velocity was for 5% methane concentration, which was 63 m s^{-1} at 12.5 m. It was noticed that the flame velocity accelerated as the length of the RS was increased. Fig. 12(b) shows the methane flame velocity at 25 m RS length. In a similar behaviour to the pressure rise, the flame velocities at 12 m and 25 m RS lengths at a stoichiometric concentration were similar in magnitude. This indicates that the developing pressure wave from the beginning of the tube works on pushing out the excess methane through the last section of the DT. The flame velocity at 5% methane concentration, however, when increasing the RS length from 12 m to 25 m, significantly accelerated the flame velocity from 70 m s^{-1} to about 83 m s^{-1}. Finally, Fig. 12(b) indicates that the flame velocity for 5% and 15% started to decelerate after 15 m. This is attributed to either consumption of fuel or the concentration not adequate to sustain the developing flame. However, 9% flame concentration was enough to maintain the acceleration of flame velocity along the DT.

The pressure wave is usually ahead of the flame due to the compression wave of the combustion products and the high pressure due to the compression wave will ignite the fuel, causing flame to reach the head of the pressure wave. The results of the current work showed that the pressure wave was ahead of the flame in all scenarios and methane concentrations (see Fig. 13).

For a greater understanding of the flame and pressure wave travelling characteristics, the interaction between flame combustion and the pressure wave pressure rise should be clarified. Fig. 13 shows the pressure and flame intensity signal for the 25 m RS for 5%, 9.5% and 15% methane concentrations. The data represents the pressure transducer and photodiode readings at five sections (Sections 2, 4, 6, 8 and 10). The red dashed lines represent the boundary of the flame's velocity (flame front) and the dashed black line represents the first peak of the pressure wave. Fig. 13 shows the front flames detected for 5%, 9.5% and 15% methane concentrations at 80 ms, 68 ms and 62 ms, respectively. As the flame velocity in the early stage is relatively low due to the low burning rate, a slow pressure wave velocity was generated. This fact made both the flame velocity and pressure wave close of each other, especially at the beginning of flame deflagration, continuing up to Section 4.

Accordingly, this section focuses on the flame front and the pressure wave in Section 4 to the end of tube. Fig. 13(a) shows the pressure and flame intensity signal for a 5% methane concentration. The pressure wave was ahead of the front flame by about 15 ms at Section 4. The last flame was detected at Section 8 and it showed that the flame followed the head pressure wave, offset by about 78 ms. Addressing the time is important to predict the location of the flame during an explosion propagation. The distance between the front flame and the head of the pressure wave at Section 4 was 1.35 m. The distance between the flame front and the head of the pressure wave at the flame extinguishment point (Section 8) was 7.02 m. Fig. 13(b) shows the pressure and flame intensity signal for a 9.5% methane concentration. The head pressure wave at Section 4 was faster than the front flame by about 15 ms (1.3 m). At Section 6, the time between the flame front and the head pressure wave was almost constant at 15 ms. However, the distance was slightly longer (1.72 m) as the flame's velocity accelerated. At Section 8, the difference between the flame front and the head pressure wave was about 27 ms, which was less than half the period, as compared to 78 ms for 5% methane concentration at Section 8. The distance between the flame front and the head pressure wave at Section 10 was about 5.6 m. The blue cycle refers to the pressure wave reflection, and the reflection of the pressure wave is clear at a 9.5% methane concentration due to a significant rise in the pressure at this concentration. Fig. 13(b) shows the pressure and the flame intensity signal for a 15% methane concentration. At Section 4, the front flame was 12 ms behind the head pressure wave, about 1.08 m distance. This value is very close to the scenarios of 5% and 9.5% methane concentrations. Within the first two sections, the distance between the flame front and the head pressure wave was 3.78 m. At Section 8, the gap between the flame front and the pressure wave were twofold, and reached about 8.1 m.

4. Conclusion

The pressure rise, stagnation pressure, and flame characteristics have been investigated in a large scale DT. The influences of the methane concentrations (from lean to the rich limit) and the variations of the RS lengths were addressed. This data will

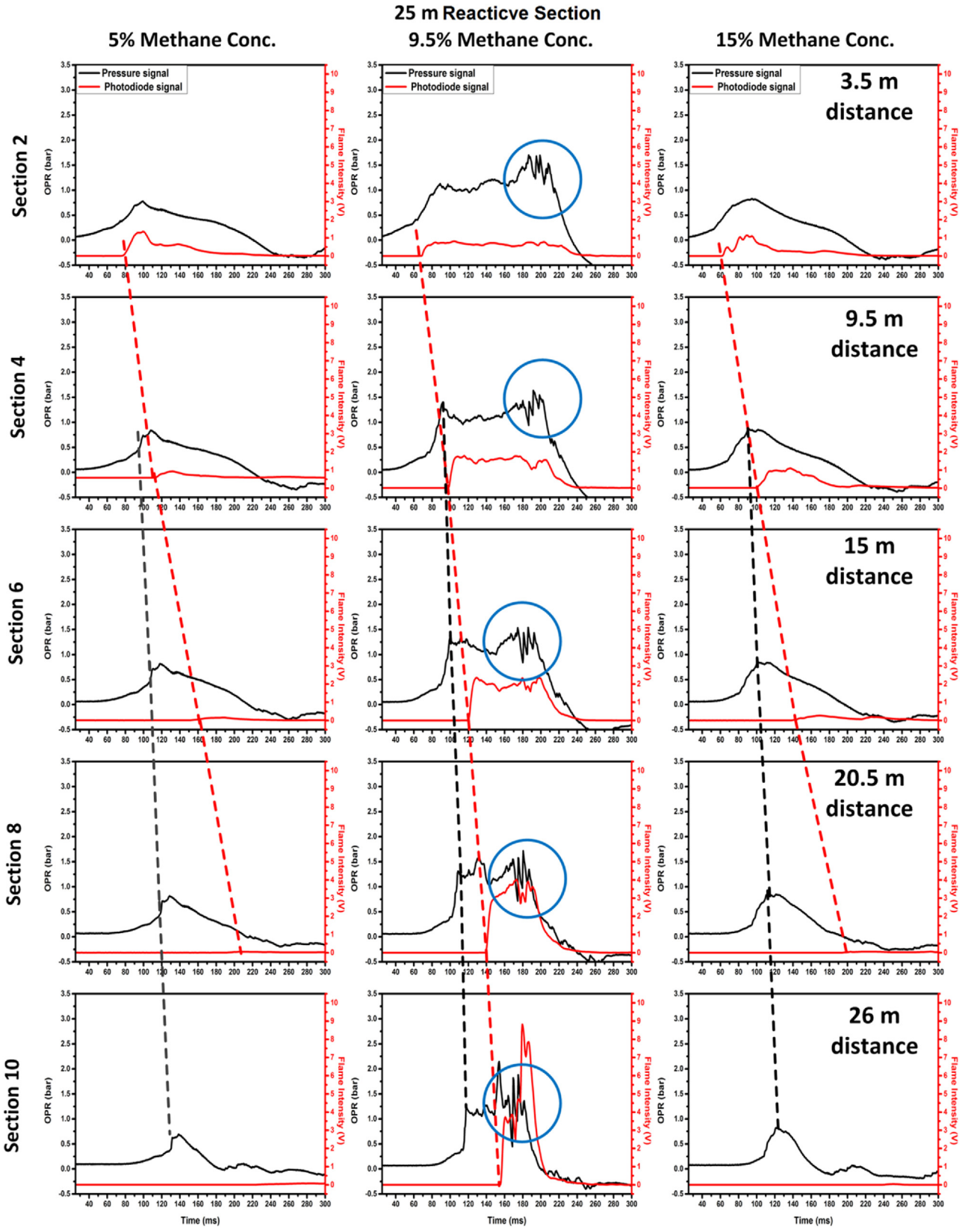

Fig. 13 – Pressure and flame intensity signal profiles for five sections of (a) 5% methane, (b) 9.5% methane, and (c) 15% methane. The red dashed line represents the flame velocity reference line, the black dashed line represents the peak pressure wave and the blue circle is the reflected wave.

assist in designing and developing the measures required for an affective alarm and mitigation system in chemical plants, and in particular in VAM capture ducts. The conclusions can be summarised in the following points:

- The explosion of 9.5% methane concentration in an explosion chamber (first section) via 50 mJ chemical ignitors released a pressure wave detected along the tube, and the flame travelled 8.5 m into the non-reactive system.
- The stagnation pressure gradually increased with an increasing RS length, from 3 m to 6 m, then 12 m. How-

ever, no significant increase in the pressure was observed as the RS length was increased from 12 m to 25 m. the maximum stagnation pressures recorded were about 4.56 bar and 4.55 bar at the 12 m and 25 m RS lengths, respectively. The maximum dynamic pressure recorded was 2.56 bar at a 9.5% concentration for a 12 m RS length and the maximum side on pressure was higher than the side on pressure in all the other results. The side on pressure significantly increased about threefold as the reactive side length was increased from 6 m to 12 m at a 9.5% concentration; however, there was a slight increase in the side on pressure as a result of increased RS lengths, from 3 m to 6 m, and from 12 m to 25 m.

- Three pressure profiles appeared in the pressure wave profiles. The first occurred at a low RS length (3 m), where the pressure wave travelled for a distance at the same pressure value and then declined at a distance dependent on the methane concentrations. The maximum pressure rise recorded was about 2 bar at 9.5% methane concentration. The second pressure profile was present for RS length from 6 m to 25 m, the pressure gradually developed at a certain distance before declining. This is clearly shown for 7.5% methane concentration at a RS length of 6 m, where the pressure developed from 1.62 bar to 2.02 bar at a distance of 12.5 m to 17.5 m, then gradually declined. This was also shown by the pressure developed for a 7.5% methane concentration and a 12 m RS length, where the pressure developed from 1.65 bar, at a distance of 12.5 m to 2.36 bar at a distance of 23.5 m, then gradually declined. The second pressure profile further showed, more significantly, by the pressure developed at 7.5% methane concentration and a 25 m RS length, where the pressure developed from 1.95 bar at a distance of 12.5 m to 2.8 bar at a distance of 23.5 m, before gradually declining. The last pressure profile pattern was distinct for 9.5% methane concentration at 12 m and 25 m RS lengths. The pressure travelled at about 2 bar along the tube, then after 23.5 m the pressure suddenly developed to a pressure in the range of 5 bar–3.75 bar at 28.5 m. The last pressure wave was attributed to the development of a flame from the deflagration to a fast deflagration or predestination stage.
- The pressure wave velocity gradually developed from the initial ignition point to the last section of the DT. The values of the velocities at the last section of DT were dependent on the RS length. For instance, at 9.5% methane concentration, the maximum pressure wave velocity increased from 177 m s^{-1} to 312 m s^{-1} as the RS length was increased from 3 m to 25 m, respectively.
- The flame was able to reach the end of the tube at 7.5% and 9.5% methane concentrations when the RS length was 3 m. The shortest flame travel distance was 9.5 m distance at 1.25% and 2.5% methane concentrations. For the 3 m and 6 m RS lengths, the flame travelled at a low intensity signal the diminished by reaching 0.05 V. At low methane concentrations (1.25%, 2.5% and 5%), however, the travelling flame had a low and constant intensity producing a signal of about 0.43 V, and increased to 1.5 V for the 7.5% and 9.5% methane concentrations. Due to the flame's acceleration and turbulence, the flame intensity signal gradually increased to 9 V at the last section of the DT for 9.5% methane concentration and 25 m RS length.
- The flame velocity showed two patterns. The first pattern was summarised as the flame starting to develop, then reaching a plateau or declining. This pattern was distinct for the 3 m RS length and for 1.25%, 2.5%, 5% and 15% methane concentrations at 6 m, 12 m and 25 m RS lengths. The second pattern observed was when the flame velocity continued to develop until reaching the last section of DT. The second pattern was distinct for a 9.5% methane concentration at distances of 12 m and 25 m. The maximum flame velocity was in the range of 162 m s^{-1}–170 m s^{-1} for a 9.5% methane concentration for the 12 m and 25 m RS length. However, the highest magnitude of flame velocity for 9.5% methane concentration was 105 m s^{-1} at a RS length of 3 m.
- The pressure wave was ahead of the flame front in all scenarios where both the methane concentrations and the lengths of the RS were varied. Nonetheless, the methane concentration plays an important role on the flame travel distance and the pressure wave along the DT. The distance between the flame velocity and the head of the pressure wave significantly reduced as a stoichiometric methane concentration was reached, where the distance at Section 8 declined by about 42% as the methane concentration was increased from 5% to 9.5%.

Acknowledgments

The authors wish to acknowledge the financial support provided to them by Australian Coal Association Low Emission Technologies Ltd (ACALET), the Australian Department of Industry, the University of Newcastle, Australia. In addition, the authors acknowledge both the Higher Committee for Education Development (HCED) and the Midland Refineries Company (MRC), Iraq for sponsoring the postgraduate researcher who working in this project.

References

Abel, F., 1869. Contributions to the history of explosive agents. Philos. Trans. R. Soc. Lond. 159, 489–516.
Ajrash, M.J., Zanganeh, J., Moghtaderi, B., 2017. The flame deflagration of hybrid methane coal dusts in a large-scale detonation tube (LSDT). Fuel 194, 491–502.
Ajrash, M.J., Zanganeh, J., Moghtaderi, B., 2016a. Experimental investigation of the minimum auto-ignition temperature (MAIT) of the coal dust layer in a hot and humid environment. Fire Saf. J. 82, 12–22.
Ajrash, M.J., Zanganeh, J., Moghtaderi, B., 2016b. Methane-coal dust hybrid fuel explosion properties in a large scale cylindrical explosion chamber. J. Loss Prev. Process Ind. 40, 317–328.
Ajrash, M.J., Zanganeh, J., Moghtaderi, B., 2016c. Effects of ignition energy on fire and explosion characteristics of dilute hybrid fuel in ventilation air methane. J. Loss Prev. Process Ind. 40, 207–216.
Akgun, M., 2015. Coal mine accidents. Turk. Thorac. J. 16, 1–2.
Amyotte, P.R., Wilkie, K.I., Mintzb, J., Peg, M.J., 1991. Effects of methane admixture, particle size and volatile content on the dolomite inerting requirements of coal dust. J. Hazard. Mater. 27, 187–203.
Bai, C., Gong, G., Liu, Q., Chen, Y., Niu, G., 2011. The explosion overpressure field and flame propagation of methane/air and methane/coal dust/air mixtures. Saf. Sci. 49, 1349–1354.
Berthelot, M., Vieille, P., 1881. Sur la vitesse de propagation des phenomenes explosifs dans les gaz. C. R. Acad. Sci. Paris 93, 18–22.
Bjerketvedt, D., Bakke, J.R., Van Wingerden, K., 1997. Gas explosion handbook. J. Hazard. Mater. 52, 1–150.
Blanchard, R., Arndt, D., Grätz, R., Scheider, S., 2011. Effect of ignition position on the run-up distance to DDT for hydrogen–air explosions. J. Loss Prev. Process Ind. 24, 194–199.

Cashdollar, K.L., Weiss, E.S., Greninger, N.B., Products, F.M., Box, P.O., Springs, B., 1992. Explos. Res. 11, 247–255.
Cashdollar, K.L., Zlochower, I.A., Green, G.M., Thomas, R.A., Hertzberg, M., 2000. Flammability of methane, propane, and hydrogen gases. J. Loss Prev. Process Ind. 13, 327–340.
Dhillon, B.S., 2010. Global mine accidents. Mine Saf. A Mod. Approach, 59–71.
Eckhoff, R., 2013. Explosion Hazards in the Process Industries. Elsevier.
Frank, L.P., 2012. Explosion, Hazard Identification, Assessment and Control. Loss Prevention in the Process Industries. Butterworth-Heinemann.
Gamezo, V.N., Zipf, R.K., Sapko, M.J., Marchewka, W.P., Mohamed, K.M., Oran, E.S., Kessler, D.A., Weiss, E.S., Addis, J.D., Karnack, F.A., Sellers, D.D., 2012. Detonability of natural gas-air mixtures. Combust. Flame 159, 870–881.
Gunther, R., Janisch, G., 1972. Measurements of burning velocity in a flat flame front. Combust. Flame 19, 49–53.
Jiang, B., Su, M., Liu, Z., Cai, F., Yuan, S., Shi, S., Lin, B., 2016. Effects of changes in fuel volume on the explosion-proof distance and the multiparameter attenuation characteristics of methane-air explosions in a semi-confined pipe. J. Loss Prev. Process Ind. 39, 17–23.
Jouguet, E., Chapman, 1913. Sur l'onde explosive. C. R. Acad. Sci. Paris 156, 872–875.
Keshavarz, M., Oftadeh, M., 2002. A new correlation for predicting the Chapman–Jouguet detonation pressure of CHNO explosives. High Temp. Press. 34, 495–497.
Kessler, D.A., Gamezo, V.N., Oran, E.S., 2010. Simulations of flame acceleration and deflagration-to-detonation transitions in methane-air systems. Combust. Flame 157, 2063–2077.
Khan, F.I., Abbasi, S.A., 1999. Major accidents in process industries and an analysis of causes and consequences. J. Loss Prev. Process Ind. 12, 361–378.
Kindracki, J., Kobiera, A., Rarata, G., Wolanski, P., 2007. Influence of ignition position and obstacles on explosion development in methane-air mixture in closed vessels. J. Loss Prev. Process Ind. 20, 551–561.
Knystautas, R., Lee, J.H., Guirao, C.M., 1982. The critical tube diameter for detonation failure in hydrocarbon-air mixtures. Combust. Flame 48, 63–83.
Kogarko, S.M., 1958. Detonation of methane-air mixtures and the detonation limits of hydrocarbon-air mixtures in a large-diameter pipe. Sov. Phys.: Techn. Phys. 3, 1904–1916.
Kundu, S., Zanganeh, J., Moghtaderi, B., 2016. A review on understanding explosions from methane-air mixture. J. Loss Prev. Process Ind. 40, 507–523.
Kuznetsov, M., Alekseev, V., Yankin, Y., Dorofeev, S., 2002a. Slow and fast deflagrations in hydrocarbon-air mixtures. Combust. Sci. Technol. 174, 157–172.
Kuznetsov, M., Ciccarelli, G., Dorofeev, S., Alekseev, V., Yankin, Y., Kim, T.H., 2002b. DDT in methane-air mixtures. Shock Waves 12, 215–220.
Lee, H., 2003. A reflection on the Mt Kembla disaster. Illawarra Unity: J. Illawarra Branch Aust. Soc. Study Labour Hist. 3, 33–45.
Li, Q., Lin, B., Jian, C., 2012. Investigation on the interactions of gas explosion flame and reflected pressure waves in closed pipes. Combust. Sci. Technol. 184, 2154–2162.
Lowesmith, B.J., Hankinson, G., 2013. Large scale experiments to study fires following the rupture of high pressure pipelines conveying natural gas and natural gas/hydrogen mixtures. Process Saf. Environ. Prot. 91, 101–111.
Mallard, E., Le Chatelier, H., 1881. Sur les vitesses de propagation de l'inflammation dans les me langes gazeux explosifs. C. R. Acad. Sci. 93, 145–148.
Market, M.T., Insight, C., In, L., Demo, R., Market, A., Insight, C., 2015. The world's worst coal mining disasters. Min. Technol., 1–7.
Mason, W., Wheeler, R.V., 1920. The propagation of flame in mixtures of methane and air. Part I. Horizontal propagation. J. Chem. Soc. Trans. 117, 36–47.
Mason, W., Wheeler, R.V., 1917. The "uniform movement" during the propagation of flame. J. Chem. Soc. Trans. 111, 1044–1057.
Moen, I.O., Lee, J.H.S., 1982. Pressure development due to turbulent flame propagation in large-scale methane-air explosions. Combust. Flame 52, 31–52.
Oran, E.S., Gamezo, V.N., Kessler, D.A., 2011. Deflagrations, Detonations, and the Deflagration-to-Detonation Transition in Methane-Air Mixtures.
Oran, E.S., Gamezo, V.N., Zipf Jr, R.K., 2015. Large-scale experiments and absolute detonability of methane/air mixtures. Combust. Sci. Technol. 187 (1–2), 324–341.
Otsuka, T., Saitoh, H., Mizutani, T., Morimoto, K., Yoshikawa, N., 2007. Hazard evaluation of hydrogen-air deflagration with flame propagation velocity measurement by image velocimetry using brightness subtraction. J. Loss Prev. Process Ind. 20, 427–432.
Payman, W., Charles, W., Shepherd, F., 1937. Explosion waves and shock waves, quasi-detonation in mixtures of methane and air. Proc. R. Soc. Lond. Ser. A: Math. Phys. Sci., 348–367.
Peraldi, O., Knystautas, R., Lee, J.H., 1988. Criteria for transition to detonation in tubes. Symp. Combust. 21, 1629–1637.
Phylaktou, H., Andrews, G., Herath, P., 1990. Fast flame speeds and rates of pressure rise in the initial period of gas explosions in large L/D cylindrical enclosures. J. Loss Prev. Process Ind. 3, 355–364.
Porowski, R., Teodorczyk, A., 2013. Experimental study on DDT for hydrogen-methane-air mixtures in tube with obstacles. J. Loss Prev. Process Ind. 26, 374–379.
Rasbash, D.J., Rogowski, Z.W., 1960. Gaseous explosions in vented ducts. Combust. Flame 84, 301–312.
Salzano, E., Marra, F.S., Russo, G., Lee, J.H.S., 2002. Numerical simulation of turbulent gas flames in tubes. J. Hazard. Mater. 95, 233–247.
Sanchirico, R., Di Benedetto, A., Garcia-Agreda, A., Russo, P., 2011. Study of the severity of hybrid mixture explosions and comparison to pure dust–air and vapour–air explosions. J. Loss Prev. Process Ind. 24, 648–655.
Sovacool, B.K., 2008. The costs of failure: a preliminary assessment of major energy accidents, 1907–2007. Energy Policy 36, 1802–1820.
Tien, J.H., Matalon, M., 1991. On the burning velocity of stretched flames. Combust. Flame 84, 238–248.
Tu, J., 2011. Industrial Organization of the Chinese Coal Industry. Freeman Spogli Institute for International Studies.
Valiev, D.M., Bychkov, V., Akkerman, V., Eriksson, L.E., 2009. Different stages of flame acceleration from slow burning to Chapman-Jouguet deflagration. Phys. Rev. E: Stat. Nonlinear Soft Matter Phys. 80, 1–11.
Wang, L., Cheng, Y.P., Liu, H.Y., 2014. An analysis of fatal gas accidents in Chinese coal mines. Saf. Sci. 62, 107–113.
Wang, Q., Ma, H., Shen, Z., Guo, Z., 2013. Numerical simulation of premixed methane-air flame propagating parameters in square tube with different solid obstacles. Procedia Eng. 62, 397–403.
Wei, H., Gillies, W.A.D.S., Oberholzer, J.W., Davis, R., 2009. Australian sealing practice and use of risk assessment criteria—ACARP project C17015. In: Proceedings of the Queensland Mining Industry Health and Safety Conference, Queensland, Australia, pp. 23–26.
Wolanski, P., Kauffman, C.W., Sichel, M., Nicholls, J.A., 1981. Detonation of methane-air mixtures. Symp. Combust. 18, 1651–1660.
Yuan, C., Amyotte, P.R., Hossain, M.N., Li, C., 2014. Minimum ignition temperature of nano and micro Ti powder clouds in the presence of inert nano TiO_2 powder. J. Hazard. Mater. 275, 1–9, http://dx.doi.org/10.1016/j.jhazmat.2014.04.047.
Zhang, Q., Pang, L., Zhang, S.X., 2011. Effect of scale on flame speeds of methane-air. J. Loss Prev. Process Ind. 24, 705–712.
Zipf, R.K., Gamezo, V.N., Mohamed, K.M., Oran, E.S., Kessler, D.A., 2014. Deflagration-to-detonation transition in natural gas-air mixtures. Combust. Flame 161, 2165–2176.